Nuclear Instruments and Methods 176 (1980) 39–50

TECHNOLOGY OF DRIFT CHAMBERS

D. SCHMIDT
Gesamthochschule Wuppertal, Wuppertal, Germany

The technical realization of wire chambers, starting from physical principles, is discussed. Problems specific to different chamber types are emphasized.

1. Introduction

In the last 10 to 15 years starting from the pioneering work of Charpak and coworkers the use of drift chambers has steadily increased in various experiments. Large complex arrangements are common in high energy set ups nowadays. Various different types were developed in the past and today, it seems to me that even new series of gaseous detectors are in the testing stage, for example parallel plate structures. muligaps and so on.

In this paper I would like to discuss only those types which have already been used in large quantities in experimental arrangements and have shown their reliability.

The conventional drift chambers to which I will restrict myself have now reached a rather high stage of development. I would like to summarize various techniques being used in chamber construction. Two examples of cylindrical chambers will be shown, one working at normal and the other at high pressure. Besides these a high resolution planar chamber will be discussed. At the end of this paper I would like to present a poor man's chamber which is inexpensive but still maintains a resonable spatial resolution. This type is suitable for large aera experiments detecting muons.

But before going into details of the chamber construction I would like to discuss the theoretical accuracy of the position measurements because this determines how carefully the chambers must be built.

2. Limitation on the position measurements

For a known velocity v of the drifting electrons the position x is given by

$$x = \int_{t=t_0}^{t=t_1} v \, \mathrm{d}t \,,$$

$$v = f\left(\frac{E}{M}\right) \to f\left(\frac{E}{p}\right)_{T=\text{const}} \,,$$

where t_0 is the time of the production of primary ions by a charged/particle, t_1 is the time at which the electrons reach the sense wire, E, M, p and T are the electric field, number of molecules per cm^3, pressure and temperature, respectively. For a gas composition such that the velocity is independent of E the relation simply reduces to $x = (t_1 - t_0)v$.

What are the limiting factors in measuring the position of the primary particles? The answer to that question can be found in many articles, for example in a beautiful publication by Sauli [1].

The spatial resolution as a function of the drift path x depends mainly on four components:

$$\sigma^2(x) = \sigma^2_{\text{track}} + \sigma^2_{\text{ion}}(x) + \sigma^2_{\text{diff}}(x) + \sigma^2_{\text{electron}} \,.$$

σ_{track} depends on the physical track width which is mainly determined by the range of the produced δ electrons and the associated γ-rays. The number of electrons with kinetic energy equal to or larger than E_0 is given in first order approximation by

$$N(E > E_0) = \frac{KZ}{\beta^2 A} \rho d \left(\frac{1}{E_0} - \frac{1}{E_{\mathrm{M}}}\right),$$

where Z, A, ρ and d are the atomic number, weight, density and thickness of the gas and E_{M} is the maximum possible energy transfer in that interaction. In going to higher density (that means increasing the pressure p) the range of the δ electrons decreases but as can be seen from the formula their number increases. The resulting effect can be seen in fig. 1.

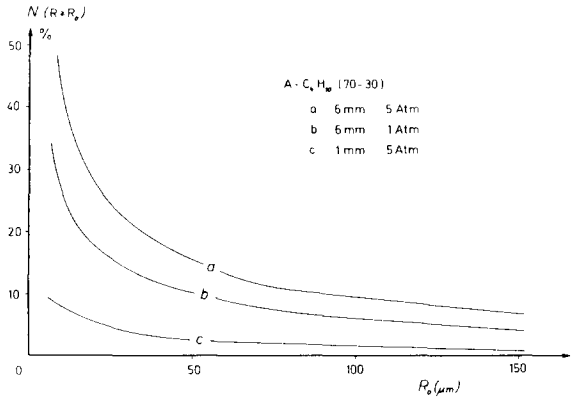

Fig. 1. Number of δ electrons with a range larger than R_0 produced by minimum ionising particles.

The curves (a) and (b) at different pressures but at the same gas volume thickness clearly show the increasing influence of the δ electrons with increasing pressure. Curve (c) shows the direct dependence of δ-ray number on chamber thickness. σ_{track} is of course independent of the drift path x.

The second term, σ_{ion}, is due to fluctuations of primary ionization density. This influences the space resolution mainly for tracks close to the sense wire. At $x = 0$ one gets $\sigma^2_{\text{ion}}(x = 0) = 1/(2N^2)$, where N is the number of primary ionization clusters per cm. When the gas pressure increases N becomes larger and σ_{ion} decreases.

The third factor, σ_{diff}, stems from the diffusion of an electron drifting along the path x

$$\Delta x = \sqrt{\left(\frac{2D}{\mu}\cdot\frac{x}{E}\right)} = f\left(\frac{p}{E}\right)\sqrt{\frac{x}{p}}.$$

D, μ are the diffusion constant and the electron mobility of the chamber gas. The effect of this diffusion will be reduced since the commonly used drift chamber electronics are almost sensitive to the first electron reaching the sense wire, making $\sigma_{\text{diff}} \approx (0.9/\ln n)\Delta x$, where n is the number of primary electrons in a cluster.

These relations show that the diffusion term contributes increasingly with the drift path x. At a constant v (that means at a constant value of p/E) the value of σ_{diff} decreases with increasing pressure p.

The last term, σ_{el}, takes into account the effects of the time measuring electronics.

Besides these statistical errors systematic deviations may contribute, for example uncertainty in the exact value of the drift velocity. But since these effects will not influence the chamber construction I will not discuss them here.

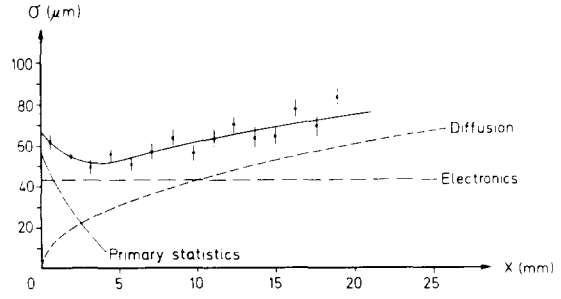

Fig. 2. Space resolution as a function of the drift length x.

Fig. 2 presents the experimentally determined track measurement error as a function of drift disdistance as measured by Sauli [1]. The increase in the error at a small drift distance due to the fluctuation of the primary statistics is clearly visible. At large x the diffusion term starts to dominate as expected.

Using higher pressures σ_{ion} and σ_{diff} decrease but σ_{track} could increase. The net effect is shown in fig. 3. These results were obtained by a group at Heidelberg [3] who did pioneering work in drift-chamber development. With increasing pressure the positioning accuracy is improved. Accuracies up to 30 μm were obtained.

What conclusions affecting chamber construction can be drawn from these considerations? Specific answers will be given in discussing the various chamber types, but as a general rule in building the most

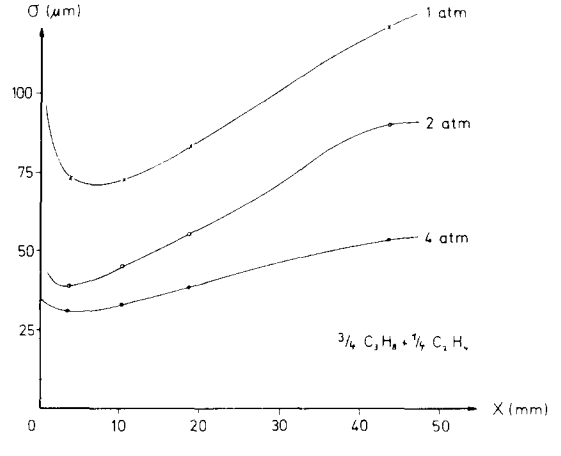

Fig. 3. Space resolution for different gas pressures.

accurate chambers with resolutions of 20–30 μm the drift path should be only a few centimeters (diffusion), the gap should be rather thin (δ electrons) and the pressure should be high.

Before going into details in describing the performance of different chamber types I would like to make some general remarks about chamber construction.

3. General principles in chamber construction

The sense wire is one of the main parts in a drift chamber. The first question is what kind of wire should be used.

The diameter should be small in order to create the high electric field needed for electron amplification. The smaller the diameter the smaller the applied voltage necessary. But there are physical limits. 20 μm is the smallest practical diameter. For long wires the ohmic resistance becomes non-negligible and attenuation of the output pulses must be considered. In fact this feature is sometimes used in determining the coordinate along the wire. For small diameters the mechanical strength also becomes a problem and larger diameters are often used. The decrease concomitant the width of the operating plateau [4] is as shown in fig. 4. Wires with 30 μm seem to be a good compromise and are the most frequently used.

In table 1 some properties of different materials are summarized.

Stainless steel wires are usually not antimagnetic due to the method of production. This prevents their use in magnetic fields. They are also difficult to solder. Gold plated tungsten wires are most frequently used to their strength properties. Since the wires are gold plated one has to be careful in soldering them. If

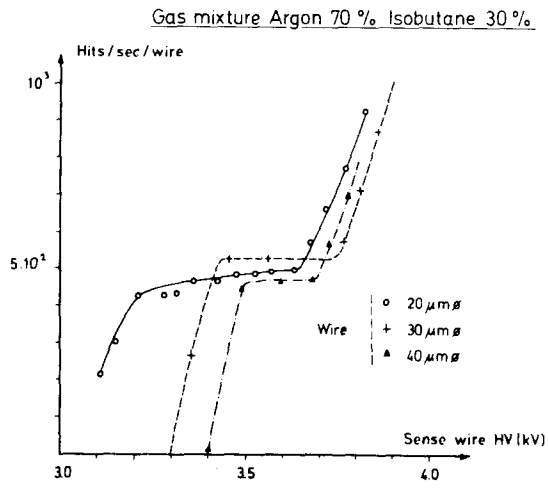

Fig. 4. Operating plateau.

the heat is too great the plating is destroyed. Therefore solder materials with low melting points (~140°C) should be used. Glueing the wire in addition makes the connection even more reliable. To avoid heating entirely the wires are often crimped.

In order to prevent the effects of electrostatic and mechanical forces from bowing the wires beyond the desired tolerances the wires are stretched during installation. The amount of load depends on the chosen material and its diameter. For example for 30 μm W it is 80 g approximately.

When dealing with thousands of wires in the same gas volume it is necessary to check each wire after it is installed. Different methods are used. By measuring the resonance frequency the tension can be checked. Another possibility is to put a small weight on the wire and to measure the elongation.

For very long wires of several meters in chambers

Table 1
Properties of several wire materials

	W (Re)	Mo	Stainless steel	Cu–Be2
Y (kP mm^{-2})	41×10^3	30×10^3	20×10^3	13×10^3
$\frac{\Delta L}{L} \cdot \frac{1}{T} \times 10^{-6}$ (°C^{-1})	4.4	5.3	16	17
Tensik strength (kP mm^{-2})	180–410	140–250	60	30–130
Remarks	most used wires		not antimagnetic	

of small thickness an additional mechanical support is often used.

A necessary condition for good track measurements is the exact positioning of the sense wire. For chambers at normal gas pressure the tolerances should be less than 100 μm. At larger pressures they should be as small as possible (10–30 μm). Different methods for positioning the wire will be shown in discussing different chamber types.

To avoid mechanical distortions with temperature variations it is desirable to use materials with almost the same expansion coefficient. Since aluminum is the usual material for support structures with an expansion coefficient of 23.8×10^{-6} per °C the choice of stainless stell and Cu–Be is favoured. If Cu–Be is tempered it loses its undesireable tendency to curl up upon breaking. If W is used the chamber should be assembled at the temperature expected during operation. In this respect the use of lucite in connection with aluminum is not the best choice. Different temperature coefficients may also cause serious troubles in making the chamber gas-tight.

In the construction of large cylindrical chambers containing several thousands of wires under stress the support structure rigidity plays a large role. I will come to that in a moment.

In assembling the chamber components special care has to be taken. The hall or the room in which this is done should be practically dust free. Otherwise the dark current will be very high. In many cases it is desirable to clean the wires with alcohol after they are installed. Kinks, of course, should be avoided; they can cause mechanical breaks. If possible each wire should be individually tested electrically. In case of high dark current temporary inversion of the wire potential often helps.

After these general remarks about constructing chambers I would like to discuss specific chambers being successfully used in experiments. Since almost every set up in high energy physics uses drift chambers I can therefore select only a few examples.

4. Cylindrical drift chambers

Cylindrical chambers usually operate in axial magnetic fields in order to measure the momenta of charged particles over a large solid angle. The momentum is determined by the curvatures of the particles in the magnetic field. To detect the particles along their tracks many layers of cylindrical chambers of high accuracy are needed.

I would like to report on two versions operating successfully.

The first is a chamber [5] constructed for a storage-ring experiment called TASSO at PETRA in Hamburg. It is in some respects similar to the central detector of MARK II at SPEAR. The dimensions of the set-up are shown in fig. 5. 15 cylindrical chambers with radii from 36 to 128 cm are built around a beam pipe having a length of approximately 350 cm. The chamber consists of about 10000 wires under stress. The support structure is appropriately rigid. It consists of two 3.5 cm thick aluminum end plates separated by a 5 mm thick inner tube of fiberglass and epoxy and a 6 mm outer cylinder of aluminum. With

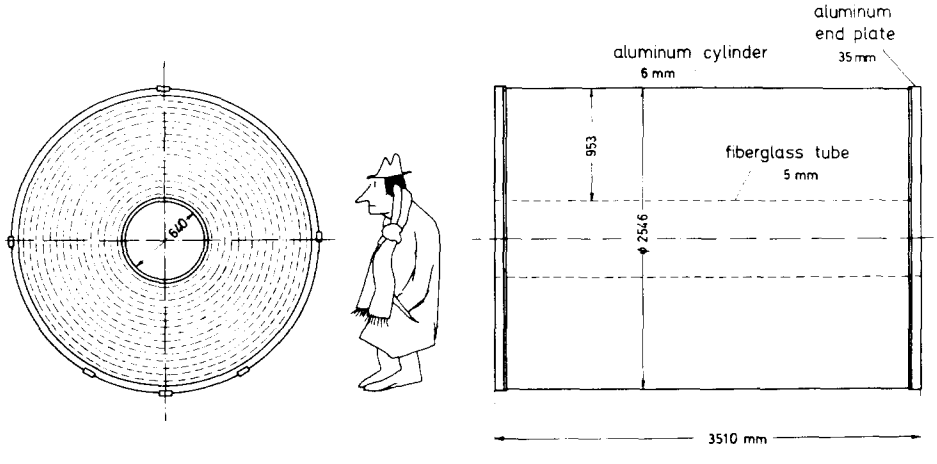

Fig. 5. Cylindrical drift chamber of the TASSO detector.

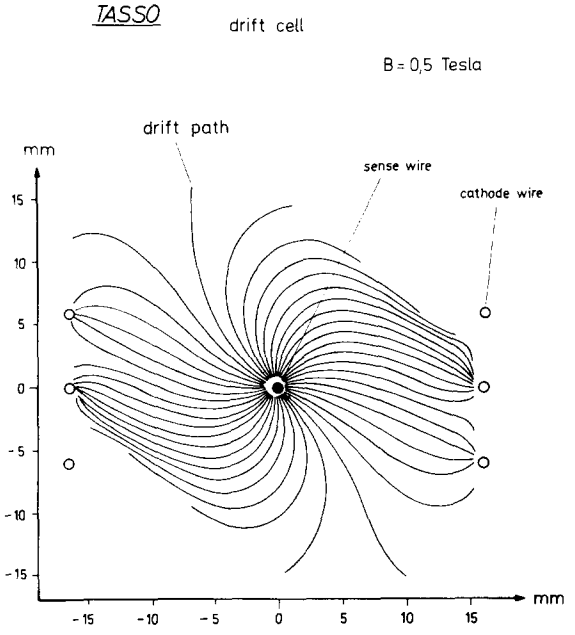

Fig. 6. Cell configuration of the TASSO chamber in a magnetic field.

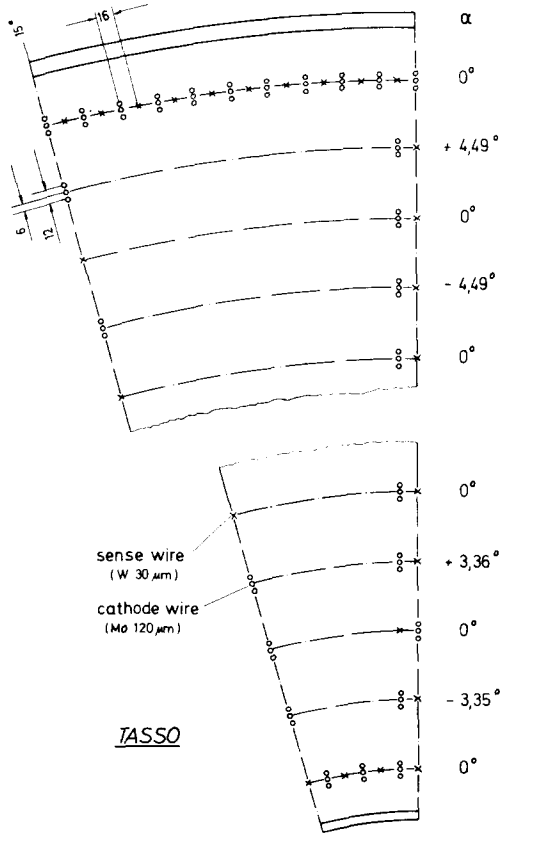

Fig. 7. Arrangement of the drift cells of the TASSO chamber.

all wires installed the distortion is less than 200 µm. The direction of the magnetic field is parallel to the cylinder axis.

The group decided to operate the chamber at atmospheric pressure. In order to obtain good spacial resolution the drift cell length should therefore be only a few cm, because at larger drift paths the effect of diffusion becomes important as I have shown in the previous section. On the other hand, since the costs of each wire are high the drift space should be as large as possible. Since the chamber has to operate in a magnetic field another factor has to be considered. The paths of the drifting electrons are affected by the magnetic field ($\boldsymbol{K}_M \sim \boldsymbol{V} \times \boldsymbol{B}$). This results in a position and angle dependent time–space relation. At a known field this can be largely corrected with special electric field configurations. Also multiple measurements of the drift time along a single particle track can be used to partly correct these magnetic effects. Since the magnetic field is relatively small in this set up (0.5 T) the authors have used the cell configuration shown in fig. 6. Three wires sitting at the same potential on each side of the sense wire are used for shaping the electric field. The black lines indicate the paths of the drifting electrons under the influence of the electric field and magnetic field.

Fig. 7 shows the arrangement of the different cell layers. To measure the coordinate parallel to the cylinder axis the wires of two neighbouring layers are tilted by a small angle. The measured resolution of this configuration is $\sigma_x = 200$ µm and $\sigma_z = 2$ mm.

What special tricks were used in constructing these chambers? Fig. 8 shows how the positioning of the wire is accomplished. The sense wire is fed through a brass tube held in an insulator. The ends of the wire are soldered and glued to a pin. The alignment of the wire is provided by a small piece which is made with 50 µm tolerance. The insulator is of high quality (Hostaform C).

The mounting of all cell components is done at constant temperature to avoid the problems of differential thermal expansion. Extreme care was taken concerning cleanliness. The technical staff wore clothes like doctors in an operating room as shown in fig. 9, which illustrates the mounting of the wires. Each wire was mechanically and electrically inspected as I have already discussed. When two, sometimes three, drift-chamber layers were completed they were covered by a 5 mm self-supporting layer of foamed lucite called Rohacell 31 with thin aluminum foils (20 µm) on each side. This protects them from being

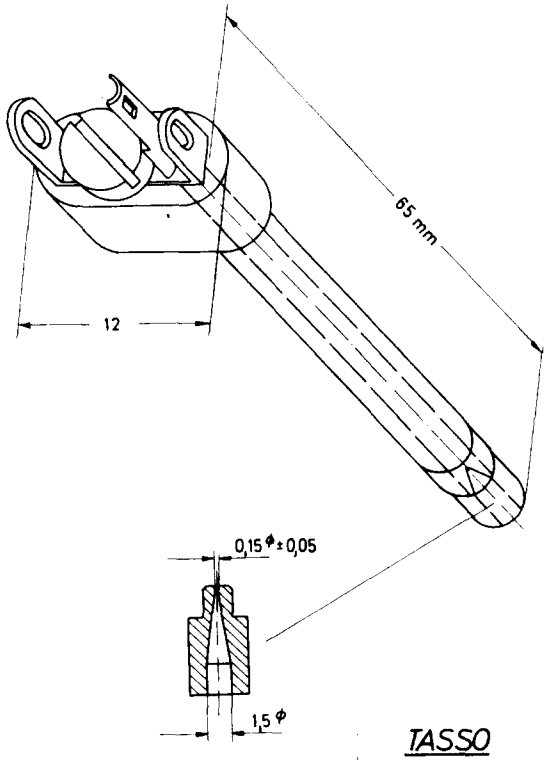

Fig. 8. Positioning of sense wire of the TASSO chamber.

destroyed or being contaminated by dust. As the density is only $\rho = 0.03$ g cm^{-3} this extra material does not effect the momentum resolution very much but alters the electric field configuration slightly.

A drift chamber set-up requiring even more accurate construction is the JET chamber built by the Heidelberg group of Heintze et al. [6] for use in the JADE experiment at PETRA.

The JET chamber is also a cylindrical chamber which operates within an magnetic field of 0.5 T, but in contrast to TASSO it is a high pressure chamber. It is specially designed to distinguish and measure large numbers of closely spaced tracks. The Heidelberg group therefore decided to use a gas mixture at 4 atm. With this increased pressure the width of the sense wire pulse decreases. Therefore particles as close as 7 mm apart can be distinguished. High pressure also reduces the influence of diffusion as we have seen in the discussion of the physical limits. This permits the use of a large drift path without losing too much in positioning accuracy. In addition dE/dx is measured to determine the specific ionisation and hence the mass of the particle. Sufficient dE/dx resolution requires that the charged primary particle produces a large number of ions in passing through the sensitive chamber volume, a requirement also helped by the high pressure.

The JET chamber consists of a pressure vessel containing 86 cells concentrated in three rings around the beam pipe (fig. 10). The length of the detector is 240 cm. To handle this configuration more easily the total surface is divided into 24 segments each containing 4 cells. Each cell has 16 sense wires (fig. 11). To ob-

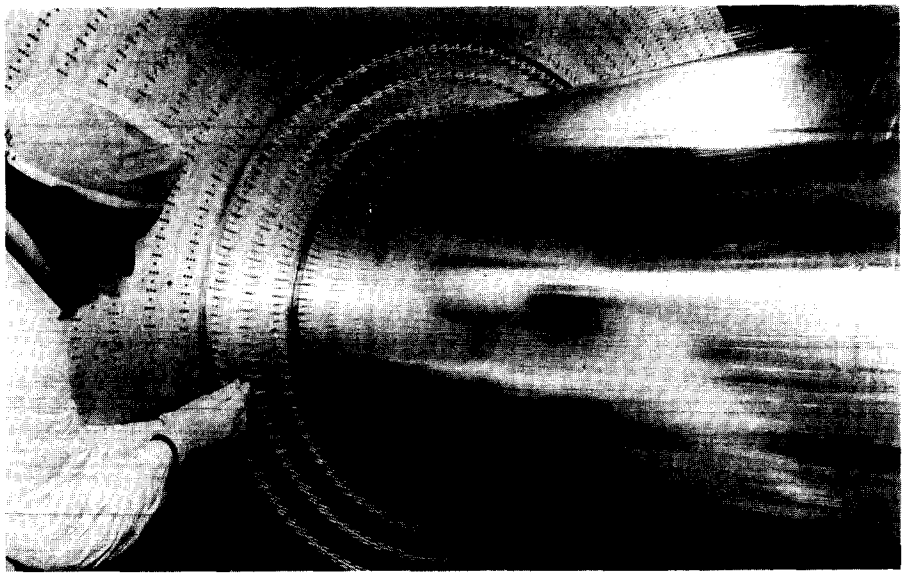

Fig. 9. Mounting of wires in the TASSO chamber.

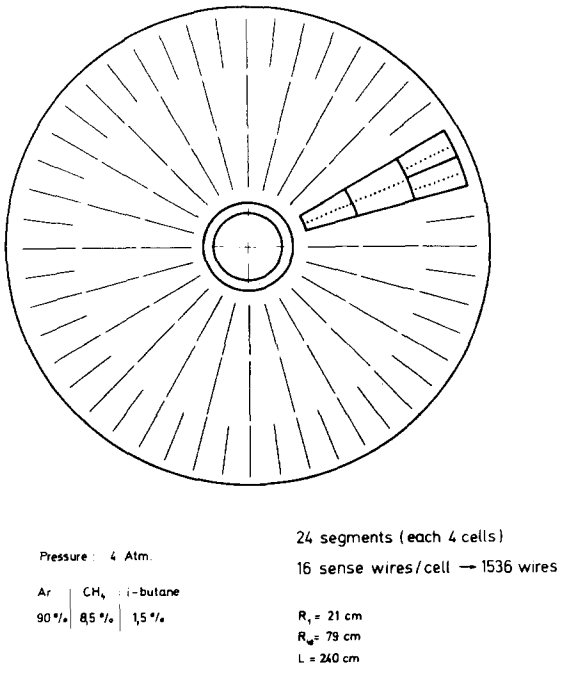

Fig. 10. Front view of detector elements of the JET chamber (JADE).

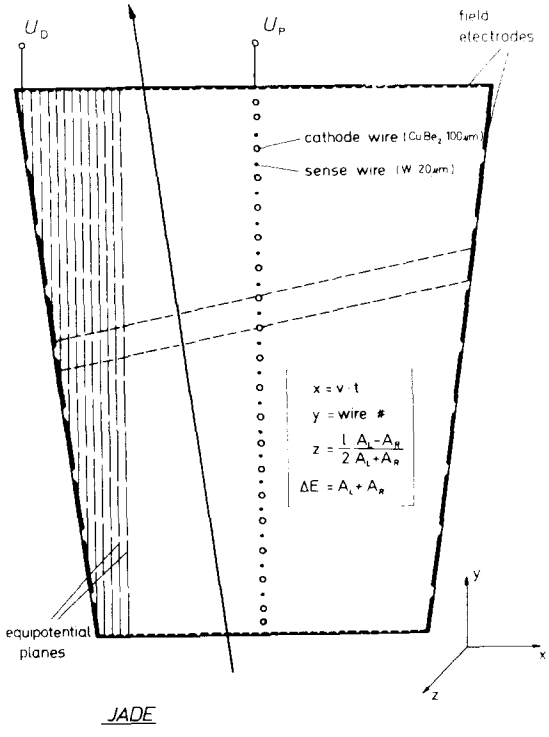

Fig. 11. Drift cell of the JET chamber.

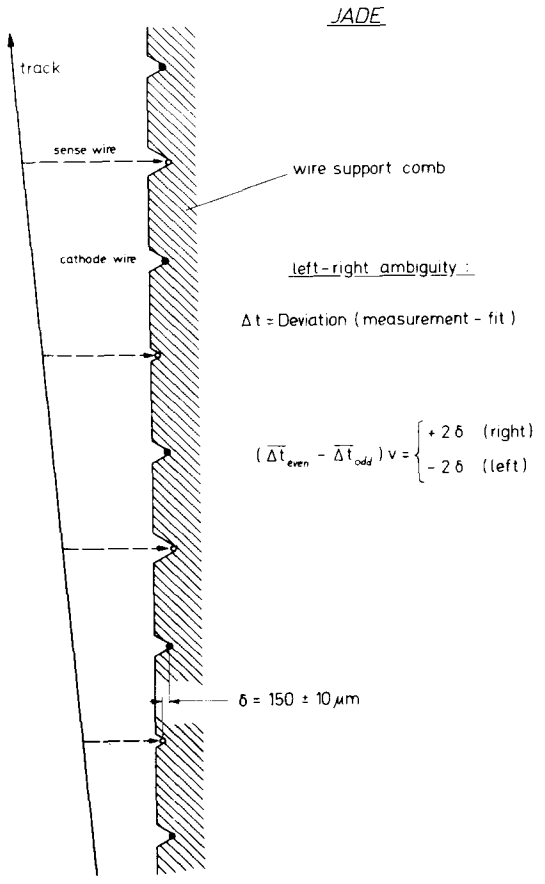

Fig. 12. Wire staggering in the JET chamber.

tain a constant electric drift field, specially aranged field electrodes on Kapton foils are placed at the cell walls. This configuration allows the measuring of the x, y, z position and the energy loss ΔE of the primary particle. x is measured by the drift time. y is determined by the position of the sense wire. The z-coordinate is obtained by the charge division method. To obtain a large value of the wire resistance they used a sense wire with a diameter of 20 μm. To determine the number of electrons produced by the primary charged particle the signals on both ends are added to correct for the attenuation.

The left-right ambiguities are resolved by staggering the wires as shown in fig. 12. Two successive sense wires are displaced alternately by a distance δ in opposite directions with respect to the cathode wires. The ambiguity is resolved by computing $(\overline{\Delta t}_{\text{even}} - \overline{\Delta t}_{\text{odd}})v = \pm 2\delta$. From the sign one can distinguish the sides. δ should be as small as possible since it can cause displacement of the wires due to the electric

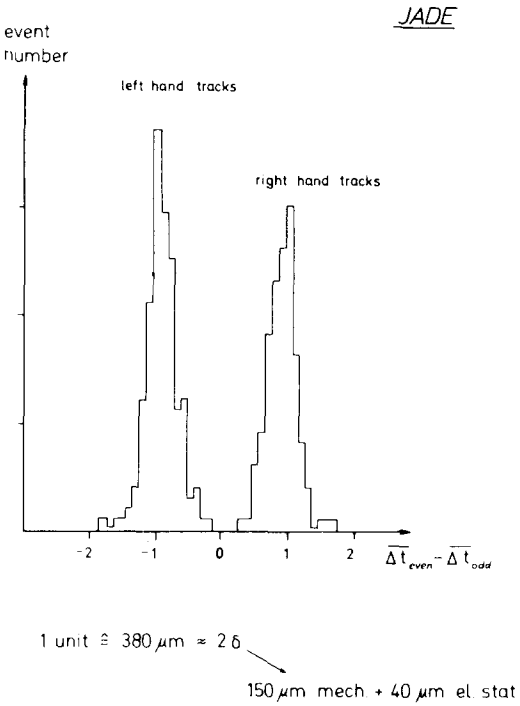

Fig. 13. Resolution of right–left ambiguity in the JET chamber.

field. It has been chosen to be 150 μm.

Fig. 13 shows the resulting resolution of the left–right ambiguity. The tracks on both sides are clearly separated. The spacial resolution is 150 μm including the effects of a 40 μm wire displacement due to electrical forces.

What are the special problems in the performance of a chamber at high pressure? Fig. 14 schematically shows the mechanical structure of a segment. The endplates, which are made of aluminum, suffer a deformation of less than 25 μm under the force of the wires. To fix the length and make the whole configuration stable, four support beams are used. To reduce the material seen by the jet particles these beams consist of a sandwich of 100 μm aluminum foils and Rohacell plexiglass foam. The straightness of this configuration is kept better than 300 μm. In order to maintain the excellent resolution and resolve the left-right ambiguity at all positions inside the chambers, all wires must sag uniformly due to gravitational forces. Using different materials and diameters the wires have to be stretched differently (60 g, 600 g, respectively). The sagging is 70 μm and the deviation for different wires is less than 7 μm. The positions of the wires are determined by notches in a machinable ceramic called Macor. The relavie accuracy of these positions in one cell is about 10 μm. The wires are soldered to a printed board mounted on the ceramic. Four brass dowels on each side of a segment guaratee that adjacent segments are aligned better than 20 μm.

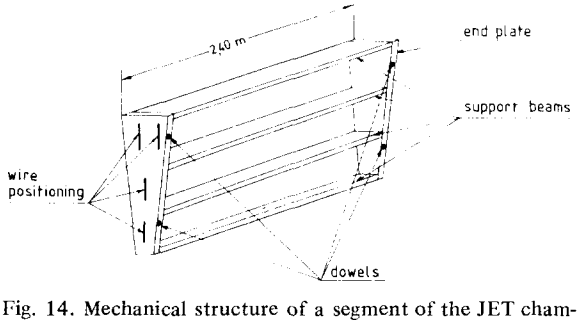

Fig. 14. Mechanical structure of a segment of the JET chamber.

The chamber was mounted under similar conditions as discussed in the TASSO set up. The JET chamber has now operated about one year and has proved its reliability. It is a good tool for looking for new physical phenomena at the PETRA storage ring.

5. Planar drift chambers

The next category of chambers I would like to discuss is the planar chamber, which is also often used in connection with magnetic fields to measure the momenta of particles. They are usually placed not in, but before and behind analyzing magnets. To assure a good momentum resolution these chambers should measure the particle track very accurately in planes separated by as much distance as possible. In order to reduce multiple scattering these chambers should also contain as little material as possible. Therefore chambers at large pressure placed inside thick wall pressure vessels cannot be used. Chambers at atmospheric pressure allow thin foils to seal the gas volume.

On example of this chamber type consists of two half circles sitting around a beam pipe. It will be built into the PLUTO forward spectrometer for measurements of $\gamma\gamma$-reactions at PETRA.

To obtain optimum spatial resolution and to tolerate the expected counting rates the drift path is chosen to be 1 cm. The thickness of a cell is also 1 cm. The left–right ambiguities are resolved by a second layer shifted by half a cell width. A second couble layer rotated by 90° measures the second

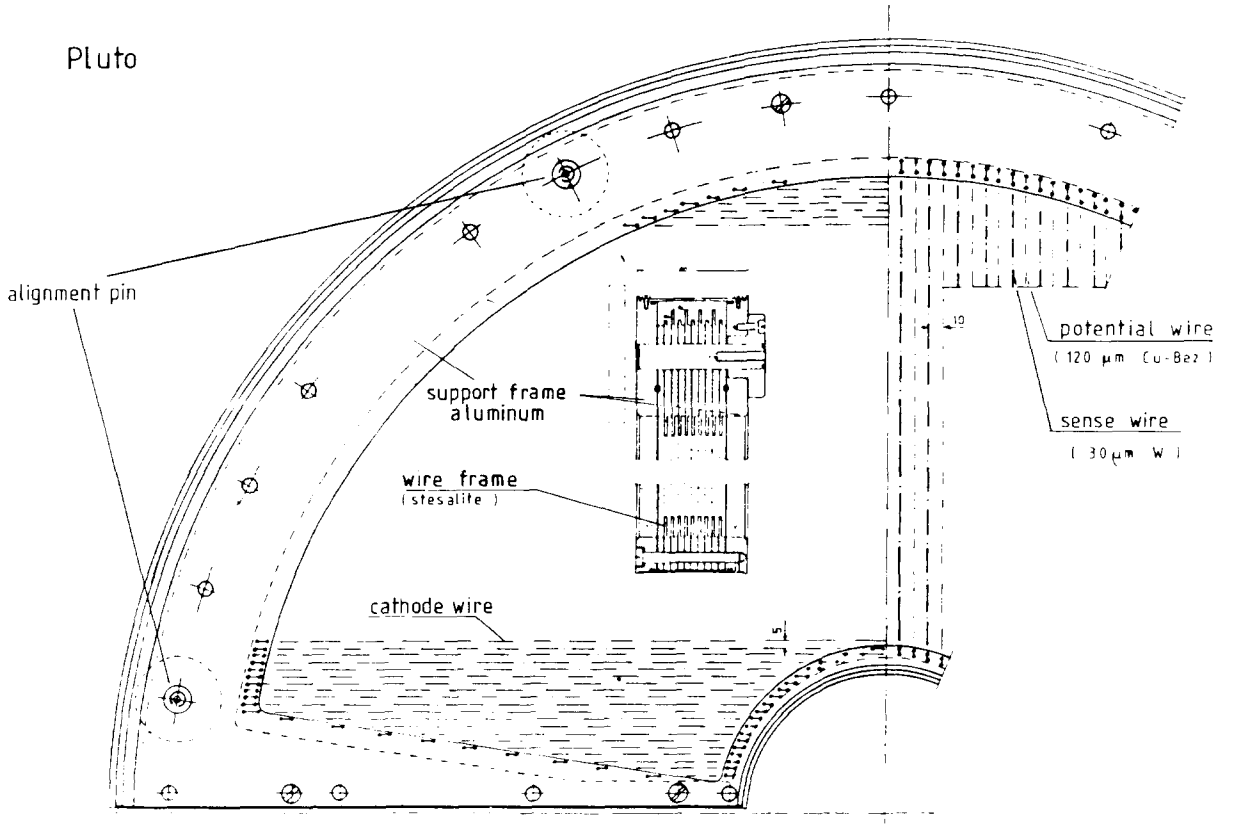

Fig. 15. Planar chamber of the PLUTO detector.

coordinate. A third double layer operating in the proportional chamber mode resolves the possible ambiguities caused by multi particles hits.

The required mechanical accuracies of about 50 μm are determined by a specially shaped 15 mm thick support frame (fig. 15). On this frame there are 4 alignment pins serving as reference points for all wire layers. The wires of each layer are soldered to an especially rigid type of printed board called Stesalite. The frame is cut out of a 5 mm solid plate which also serves as spacer between adjacent wire layers. To avoid disturbing the solder joints of the wires the printed board provides a separate pad for soldering the connection to the preamplifiers.

In high accuracy chambers it always is interesting to see which method is used to position the sense wires exactly. In this case the alignment is done by hand using the aid of a microscope on a measuring table. The cathode wires are fixed on a similar etched frame. Since these wires do not need to be as accurately positioned as the former ones they are aligned using the transfer frame technique. The spacial resolution is better than 200 μm on the average. Including the mylar foils (0.1 mm) which seal the gas volume a crossing particle sees only 4×10^{-3} radiation lengths of material.

In high energy physics large area detectors covering several hundred m^2 and having resonable space resolution are often needed. One example is a μ detector consisting of chambers placed behind a thick wall of absorbing material.

The counting rates are usually not high. The expenses for such a device can be kept low by using drift chambers with large drift cells.

Since the costs for time measuring devices are not small the amplifier output of several wires can be ored and fed into the same TDC input. An inexpensive flipflop connected to each sense wire indicates from which wire the time measurement stems.

I would like to report on such a system developed for the PLUTO detector. One of the main principles in producing these chambers was to use mass production techniques as much as possible since man power is getting more and more expensive. This also

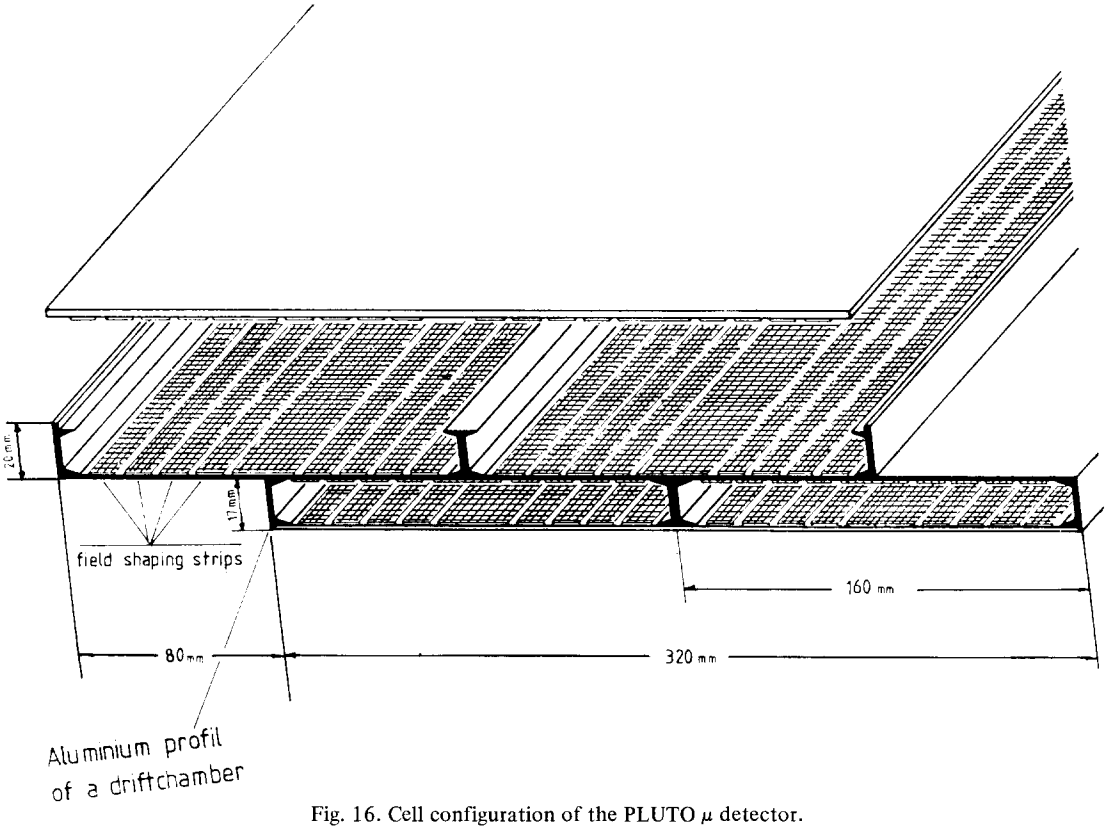

Fig. 16. Cell configuration of the PLUTO μ detector.

increases the reliability of the whole system. Each chamber consists of four drift cells arranged in two layers. The layers are displaced with respect ot each other by half the cell width to resolve the left–right ambiguities. The units are small enough to fit into almost all geometrical configurations. Smaller units would cost more for high voltage distribution and electronics. The body of the four cells is a specially designed extruded aluminum profile and is shown in fig. 16. The U and I beams on both sides of a plate guarantee a rigid structure. These profiles fix almost all dimensions. The maximum drift length is 8 cm which is determined by the repetition rate of PETRA. To be fully efficient along the whole cell the drift field must be shaped with an arrangement of conducting strips. The minimum number of strips is given by the tolerable difference of $E_{\max} - E_{\min}$ determined by the plateau of the saturated drift velocity. Fig. 17 shows that no more than 5 strips are needed.

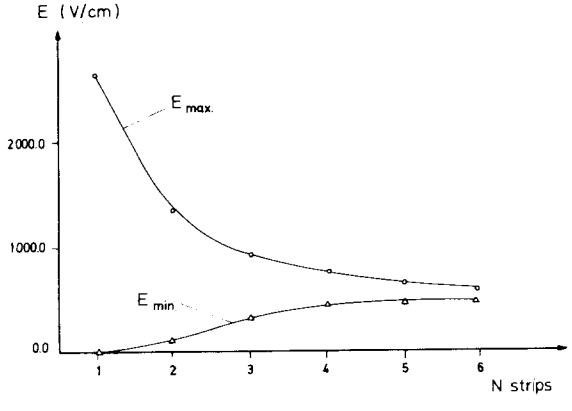

Fig. 17. The maximum and minimum electric field for different strip numbers.

Such conducting strips are often produced from printed board material (etched G10 for example). G10 is not affected by any of the known gas mixtures but it is rather expensive. To reduce the costs polystyrol sheets were employed as a support for inexpensive selfadhesive 25 μm aluminum field shaping strips. Polystyrol is a very cheap material commonly used for food containers, such as yoghurt. Extensive tests have shown that this material will not poison the chamber gas. The field shaping elements were fabri-

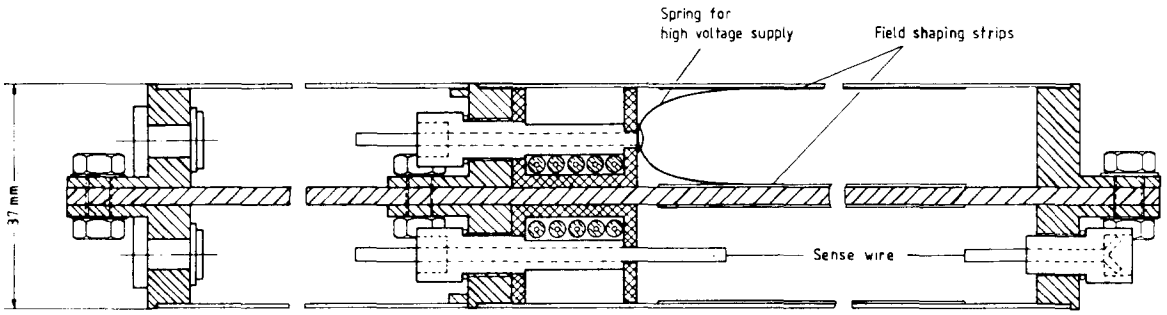

Fig. 18. Side view of the μ detector.

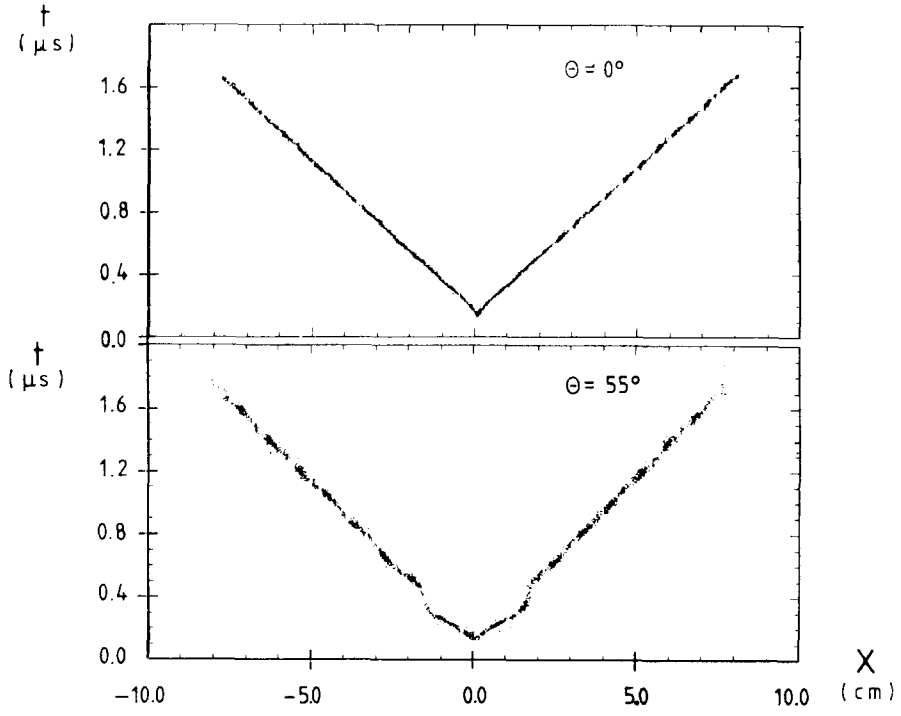

Fig. 19. Time–space relation for minimum particle of 0° and 55° incident angles.

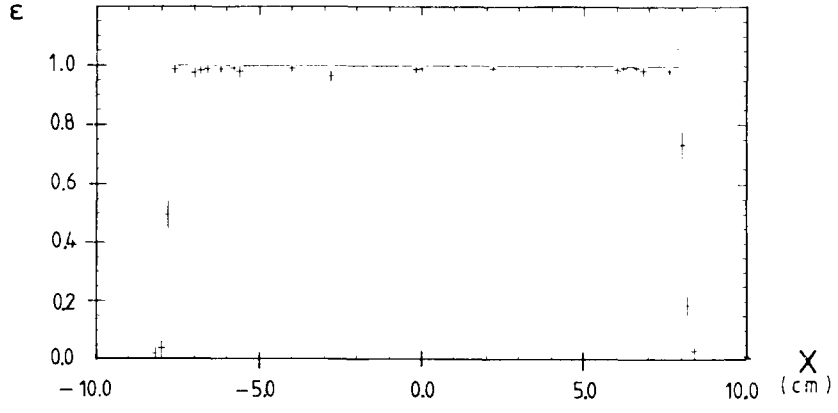

Fig. 20. Efficiency as a function of the drift path.

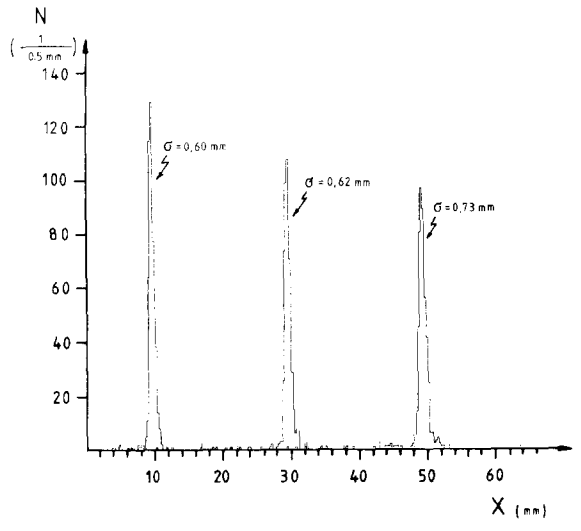

Fig. 21. Space resolution for different drift paths.

cated using mass production techniques. In glueing the field shaping elements into a cell only minimum care is needed. A 1 mm thick aluminum sheet which also holds field chaping elements is glued to the top of each double chamber.

The end pieces with the wire positioning elements and the strip voltage supply is shown in fig. 18. To avoid soldering, the connections to the strips are made by Cu–Be springs. This enables the use of inexpensive insulating materials such as Delrin which is also easier to machine. In the lower chamber the sense wire positioning is shown. The wire is soldered into a brass tube with a 0.5 mm inner diameter.

To show that such a simple configuration works satisfactorily the measured timespace relations for particles with incident angles of 0° and 55° with respect to the normal of the chamber plane are shown in fig. 19. As shown in fig. 20 the chamber has an almost 100% efficiency over the whole drift path. Fig. 21 demonstrates the resonable space resolution of the detector.

I would like to thank Prof. J. Heintze, Dr. U. Kötz and Dr. G.G. Winter for their invaluable cooperation in discussing their experimental set up. I am indebted to Dr. R. Kellogg for many discussions and for reading the manuscript. Finally I with to thank Mrs. R. Siemer and Mr. P. Burmeister for excellent technical support.

References

[1] W. Sauli, CERN 77-09.
[2] G. Schulz et al., Nucl. Instr. and Meth. 151 (1978) 413.
[3] W. Farr et al., Nucl. Instr. and Meth. 154 (1978) 175.
[4] G. Morel et al., Nucl. Instr. and Meth. 141 (1977) 43.
[5] H. Boerner et al., these proceedings, p. 151.
[6] W. Farr et all., Nucl. Instr. and Meth. 156 (1978) 283;
J. Heintze, Nucl. Instr. and Meth. 156 (1978) 227;
H. Drumm et al., these proceedings, p. 333.